An Adjustable Narrow Band Microwave Delay Equalizer

THOMAS A. ABELE AND HAN-CHIU WANG

Abstract—**A simple low loss microwave delay equalizer for the delay equalization of narrow band microwave bandpass filters has been explored. This equalizer is quite small and does not require the use of additional components such as circulators or hybrids. It exhibits a reflection coefficient of less than 1 percent and possesses two very valuable and convenient features: a continuous adjustment of the delay shape and of the center frequency.**

The structure is analyzed theoretically, an equivalent circuit is derived, and expressions for both delay and loss are given. Also presented are design data and experimental results concerning the actual delay equalization of a bandpass filter and the temperature behavior of the equalizer and the filter-equalizer combination.

I. Introduction

An improved type of microwave delay equalizer particularly suitable for the delay equalization of microwave bandpass filters has been explored.

Previous work[1] in this field has been based on the principle that the delay between the incident and the reflected wave of a lossless resonant termination possesses a shape suitable for compensating the delay distortion of a microwave bandpass filter, but to utilize this effect a hybrid or a circulator must be added to separate the two waves. Another type of equalizer has been proposed by Tillotson[2] and was also described by Cohn.[3] In contrast to the aforementioned principle, this equalizer is a simple integral 2-port structure which electrically closely resembles the well-known lattice network of lumped element network theory. In the following discussion an improved version of this type of equalizer is introduced and the theoretical and practical aspects of its design are discussed.

The reflection-type equalizer has a number of disadvantages, if compared with the structure by Tillotson and Cohn. First, it is more expensive, bulkier, and heavier because of the hybrid or circulator, whereas the other equalizer is very easy to construct and, consequently, quite inexpensive and has a very moderate size: an insertion length of four inches is sufficient for an equalizer at 4 GHz. The dissipation losses of reflection-type equalizers are always higher due to the additional losses in the hybrid or circulator. The achievable return loss of a reflection-type equalizer is limited by the return loss of the hybrid or the circulator, which commonly is close to 30 dB. A similar limitation exists for the structure by Tillotson and Cohn because of the lack of adjustments. In contrast to this, the equalizer described here is capable of providing return losses which are greater than 40 dB and, in addition, possesses an extremely valuable feature that not only the center frequency but also the shape of the delay around the center frequency can be adjusted continuously. This proved to be of great advantage for the actual process of exactly delay equalizing a given bandpass filter.

This paper is divided into two parts. The first (Section II) is devoted to the theoretical treatment of the structure. An equivalent circuit (lattice network) is derived and the conditions are given, which are necessary to make it an allpass network. Then the delay of this allpass is calculated and shown to be related to the coupling coefficient in a simple manner. Finally, a theoretical estimate is obtained for the dissipation losses and a very simple design formula is given to minimize these losses.

The second part (Section III) is devoted to experimental investigations. Starting with results obtained from some preliminary test models all major improvements are described, which led to the final configuration. Then the results of an actual delay equalization of a microwave bandpass filter are reported together with measured data concerning the temperature behavior of the equalizer as well as of the composite (filter-equalizer) structure. Finally, measured design information is presented, which should be sufficient for the delay equalization of most narrow band microwave bandpass filters.

II. Theoretical Analysis

The structure under consideration is shown in Fig. 1. A circular cavity is situated on the broad wall of a rectangular waveguide and is coupled to this waveguide by a symmetrical aperture which is oriented in such a way that the structure retains one symmetry plane. This is namely, the plane which coincides with the axis of the cavity and which is perpendicular to the longitudinal axis of the rectangular waveguide. It is assumed, that only the dominant modes propagate in the rectangular and in the circular waveguide. For the rectangular guide, this is the TE_{10} mode and for the circular guide these are the two TE_{11} modes, since the eigenvalue is doubly degenerate.

Equivalent Circuit and Its Allpass Characteristic

To analyze the structure, the scattering matrix formulation is used. The detailed analysis starting with an evaluation of the properties of the junction shown in Fig. 2 is given in the Appendix. It is shown there, that after imposing the terminal conditions at ports 3 and 4

$$a_3 = -e^{-2j\beta l_3}b_3,$$
$$a_4 = -e^{-2j\beta l_4}b_4 \qquad (1)$$

Manuscript received January 11, 1967; revised March 6, 1967 and May 12, 1967.

The authors are with Bell Telephone Laboratories, Inc., North Andover, Mass.

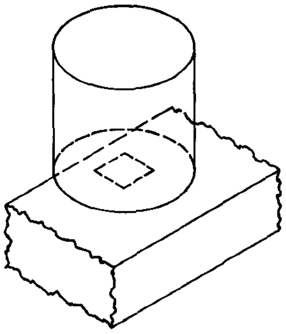

Fig. 1. Configuration of the delay equalizer.

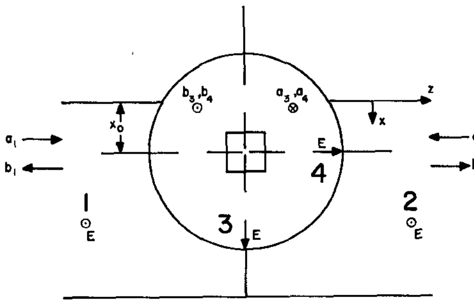

Fig. 2. Pertinent quantities of the 4-port junction.

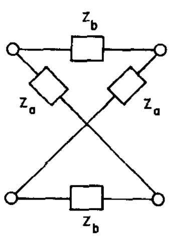

Fig. 3. The equivalent symmetrical lattice network.

the structure of Fig. 1 can be characterized by the equivalent symmetrical lattice network of Fig. 3 with the lattice impedances

$$Z_a = -j \tan(\theta_{13} - \theta_{33} + \phi + \beta l_3),$$
$$Z_b = -j \tan(\theta_{14} - \theta_{44} + \psi + \beta l_4) \qquad (2)$$

where θ_{ij} is the argument of S_{ij}, $\beta = 2\pi/\lambda_g$ is the propagation constant of the TE_{11} mode in the cavity, and where

$$\phi = \arc\tan \frac{\sin(\theta_{33} - 2\beta l_3)}{|S_{33}| + \cos(\theta_{33} - 2\beta l_3)} \qquad (3)$$

$$\psi = \arc\tan \frac{\sin(\theta_{44} - 2\beta l_4)}{|S_{44}| + \cos(\theta_{33} - 2\beta l_3)} \cdot \qquad (4)$$

One of the essential characteristics of a delay equalizer is that it must be an allpass. As again is shown in the Appendix the symmetrical lattice network of Fig. 3 *is* a matched allpass, if

$$S_{33} = S_{44} \qquad (5a)$$
$$\theta_{13} = \theta_{14} + \frac{\pi}{2} \qquad (5b)$$

and

$$l_3 = l_4 = l. \qquad (5c)$$

Equation (5c) can readily be fulfilled. However, an exact evaluation of the scattering matrix elements in order to fulfill (5a) and (5b) would be quite difficult. An approximation based on small aperture theory[4] however is easy to obtain and, as will be seen later, gives sufficiently accurate results.

In order to characterize a given coupling aperture by small aperture theory, the aperture is usually described by an electric polarizability and by two magnetic polarizabilities along two axes. Let M_x and M_z be the magnetic polarizabilities along the x and z axes, respectively (see Fig. 2). Then the desired elements of the scattering matrix can be expressed in a very simple form, as is shown in the Appendix. As is derived there, a solution to (5a) and (5b) can be achieved by choosing

$$M_x = M_z = M \qquad (6)$$

provided that x_0 (Fig. 2) satisfies the condition

$$\cos \frac{\pi x_0}{a} = \frac{2a}{\lambda_{gr0}} \sin \frac{\pi x_0}{a} \qquad (7)$$

where a is the width of the rectangular waveguide and λ_{gr} is the wavelength of the TE_{10} mode in this guide.

Group Delay

Under the conditions (5c) through (7), the allpass network possesses a group delay of the transmission coefficient (33) of the form

$$\tau = -2 \frac{d}{d\omega}(\theta_{13} - \theta_{33} + \phi + \beta l). \qquad (8)$$

For most microwave structures, the frequency band of interest is relatively narrow (≤ 1 percent relative bandwidth), hence, as is commonly done, all the elements of the scattering matrix can be considered to be independent of frequency. A further justification for this assumption based on small aperture theory is given in the Appendix. Therefore

$$\tau \approx -2\frac{d\beta l}{d\omega} - 2\frac{d\phi}{d\omega}$$
$$= \frac{1 - |S_{33}|^2}{(1 + |S_{33}|^2) + 2|S_{33}| \cos(\theta_{33} - 2\beta l)} \frac{d}{d\omega}(2\beta l)$$
$$= \mathrm{DAF} \frac{d}{d\omega}(2\beta l). \qquad (9)$$

The factor $(d/d\omega)(2\beta l)$ in (9) is the delay of a TE_{11} wave traveling through a length $2l$ in the circular waveguide. For any reasonable l this factor is quite small and frequency insensitive. Unless the first factor, called the delay amplification factor (DAF) is a large frequency sensitive term, this structure will not be useful for narrow band delay equalization. It is thus seen that $|S_{33}|$ must be made to approach unity and that the structure must be operated around a frequency f_0 corresponding to

$$\cos(2\beta_0 l - \theta_{33}) = -1. \quad (10)$$

To study the frequency behavior in the vicinity of f_0 the following substitutions are used:

$$2\beta l = 2\beta_0 l + \Delta\beta l$$

and

$$|S_{33}| = 1 - \partial$$

with $0<\partial\ll 1$. As seen from (23), $|S_{13}|$ is related to ∂ by

$$|S_{13}| = \sqrt{\partial}\,\sqrt{1-\partial/2}.$$

The delay amplification factor can then be expressed as

$$\mathrm{DAF} = \frac{1-(1-\partial)^2}{1+(1-\partial)^2 - 2(1-\partial)\cos(\Delta\beta l)} = \frac{2-\partial}{\partial}\,\frac{1}{1+\dfrac{4(1-\partial)}{\partial^2}\sin^2\dfrac{\Delta\beta l}{2}}. \quad (11)$$

This expression makes the frequency behavior of τ in the vicinity of f_0 apparent, if the small variation of $(d/d\omega)(2\beta l)$ due to frequency changes is neglected. It is seen that the curve τ versus β will be arithmetically symmetrical with respect to β_0, that it possesses a maximum at β_0 and that the value of this maximum as well as the steepness of the descent on either side of β_0 will increase, if ∂ is decreased, i.e., when the coupling is decreased. Since the general shape of τ versus β cannot be changed by any means and because of the narrow band nature of resonant cavities, the application of this structure for delay equalization is limited to certain areas. For example, it may not be suitable to equalize the delay distortion due to a long dispersive transmission line (for instance a guide not operated in a TEM mode). However, the shape of the delay curve is quite well suited for the delay equalization of narrow band microwave bandpass filters, as is already pointed out by Merlo.[1]

Dissipation Losses

Up to this point dissipation losses have not been taken into account. For the application as a delay equalizer, however, at least an estimate for these losses should be available. Furthermore, it will in general be desirable to minimize these losses.

First, an estimate for the dissipation losses of the structure shall be obtained. Since the cavity is the only resonant element, its intrinsic losses will be the major contribution. These losses consist of losses in the sidewall of the cavity, in the end plate, and in the coupling plate. Because of the complicated distribution of the surface currents in the vicinity of the aperture, it would be quite difficult to evaluate this third contribution. However, it is quite reasonable to assume that this contribution will be approximately equal to and most likely somewhat larger than the contribution of the end plate. Hence, the dissipation losses will be calculated by assuming no losses in the coupling plate and doubling the losses in the end plate. Equation (1) is therefore rewritten as

$$a_3 = -e^{-(2\alpha l+2\epsilon)}e^{-2j\beta l}b_3,$$
$$a_4 = -e^{-(2\alpha l+2\epsilon)}e^{-2j\beta l}b_4 \quad (12)$$

where $e^{-2\epsilon}$ expresses the doubled end plate losses and $e^{-2\alpha l}$ expresses the losses in the side wall of the cavity. Equation (12) shows that the considered losses may easily be computed by replacing βl in all equations by $\beta l - j(\alpha l+\epsilon)$. Since

$$\alpha l + \epsilon \ll 1$$

the new transmission coefficient S_t' can be approximated from (33) by using the first two terms of a Taylor expansion

$$S_t' = S_t(\beta l) + \left.\frac{dS_t}{d\beta l}\right|_{\beta l}\frac{1}{j}(\alpha l + \epsilon)$$
$$= S_t(\beta l)\left[1 - \tau(\beta l)\left.\frac{d\omega}{d\beta l}\right|_{\beta l}(\alpha l+\epsilon)\right]$$
$$= S_t(\beta l)\left[1 - \mathrm{DAF}(\beta l)(2\alpha l + 2\epsilon)\right].$$

For small losses ($\mathrm{DAF}(\beta l)(2\alpha l+2\epsilon)\ll 1$) this results in

$$|S_t'| \approx e^{-\mathrm{DAF}(2\alpha l+2\epsilon)}. \quad (13)$$

The assumption $\mathrm{DAF}(\beta l)(2\alpha l+2\epsilon)\ll 1$ is obviously justified for any structure of reasonable insertion loss (≤ 1 dB). It is seen from (13) that the total insertion loss of the structure is equal to the product of DAF and the return loss of the circular waveguide with end plate $(2\alpha l+2\epsilon)$, i.e., the loss suffered by a wave traveling through the circular waveguide to the end plate and back. In precisely the same manner the total delay of the structure (9) was equal to the product of the "return delay" of the circular waveguide with end plate $[(d/d\omega)(2\beta l)]$ and the same factor DAF. Insertion loss and delay of the equalizer therefore are proportional to each other with a frequency-independent proportionality factor (neglecting the small variations of $(d/d\omega)(2\beta l)$ and $2\alpha l+2\epsilon$ for the narrow frequency range of interest). This result is in agreement with the well-known general formula due to Mayer.[5]

As already mentioned, it will in general be desirable to keep the dissipation losses of the structure as small as possible. However, since it is to be used to equalize a particular delay distortion around f_0, it is necessary that the shape of the delay curve versus f is kept unchanged around f_0, while minimizing the dissipation losses. This will be achieved to a good approximation, if the second derivative $(d^2\tau/d\omega^2)$ at f_0 is kept constant, since the shape of the delay curve versus f is predominantly parabolic around f_0, as was already pointed out. With $\tau_0=\tau(f_0)$, $\lambda_{g0}=\lambda_g=(f_0)$, $\lambda_0=\lambda(f_0)$, the term [(9), (11)].

$$\left.\frac{d^2\tau}{d\omega^2}\right|_{f_0} = \tau_0^3\,\frac{1-\partial}{2(2-\partial)^2}\cdot\left[1 - \frac{\partial^2}{1-\partial}\,\frac{3}{\pi^2}\,\frac{\lambda_{g0}}{2l}\left(1 - \frac{\lambda_0^2}{\lambda_{g0}^2}\right)\right]$$

must, therefore, be kept constant. Since, as mentioned before $\partial\ll 1$, and since as a result of this ($|S_{13}| = \sqrt{\partial(1-\partial/2)}$, the

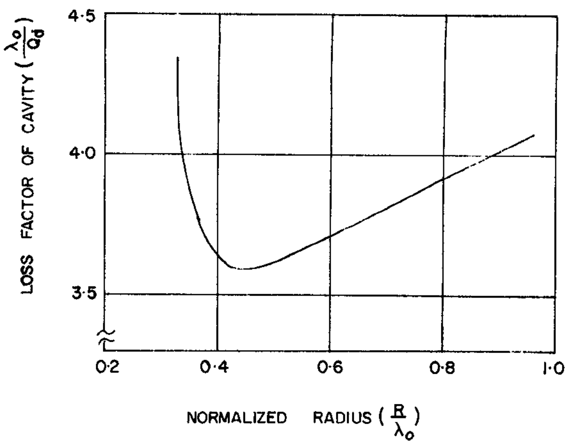

Fig. 4. Dissipation loss for various sizes of cavities.

resonator is loosely coupled resulting in $2l \approx \lambda_{g0}$. It is seen that the same result is obtained in good approximation, if τ_0 alone is kept constant. That is, the slope of the delay curve versus f around f_0 remains approximately unaltered, if τ_0 is kept constant.

Hence, in minimizing the dissipation losses, the *entire* function $\tau(f)$ will essentially remain unaltered around f_0, and it will therefore suffice to minimize the dissipation losses at f_0. This is seen from

$$\mathrm{DAF}(\beta l)(2\alpha l + 2\epsilon) \approx \frac{\tau}{\tau_0} \mathrm{DAF}(\beta_0 l)(2\alpha l + 2\epsilon)$$

which shows that by minimizing the dissipation losses at f_0, the losses are likewise minimized at any frequency in the vicinity of f_0. From (9) and (11) it is found

$$\mathrm{DAF}(\beta_0 l)(2\alpha l + 2\epsilon) = \tau_0 f_0 \lambda_{g0} \left(\frac{\lambda_0}{\lambda_{g0}}\right)^2 \left(\alpha + \frac{\epsilon}{l}\right). \quad (14)$$

A completely closed cavity of the same dimensions as the one used in the structure has an unloaded Q, according to Montgomery[6] of

$$\frac{1}{Q} = \frac{1}{\pi}\left(\frac{\lambda 0}{\lambda_{g0}}\right)^2 \lambda_{g0}\left(\alpha + \frac{2\epsilon}{\lambda_{g0}}\right). \quad (15)$$

Thus, substituting $2l \approx \lambda_{go}$ as before, it is seen that

$$\mathrm{DAF}(\beta_0 l)(2\alpha l + 2\epsilon) = \frac{\pi}{Q} f_0 \tau_0.^1 \quad (16)$$

Since both f_0 and τ_0 have to be kept constant, Q must be maximized to minimize the dissipation losses. Fig. 4 shows a plot of $(1/Q)(\lambda_0/d)$ versus R/λ_0 as obtained from Wilson *et al.*[7] R is the cavity radius and d is the skin depth as commonly derived. It is seen that the value

$$R = 0.43\lambda_0 \quad (17)$$

is optimum.

[1] To relate the dissipation losses at f_0, in this simple manner, directly to the unloaded Q of the cavity was suggested by one of the reviewers of this paper.

III. Experimental Results

Preliminary Tests

To obtain a practical configuration for an equalizer some test models were made and tested to determine which parameters of the equalizer would be most pertinent to the design of an improved model. Because of this special test purpose, the models were made so that most parts could be moved and interchanged (aperture shape, location of the coupling hole, diameter of the cavity, etc.). All tests were made in the frequency band from 3.7 to 4.2 GHz with WR229 as the rectangular waveguide.

One of the most important results obtained from these tests was information concerning the shape and size of the aperture. As mentioned in Section II the aperture must be symmetrical and it must be

$$S_{33} = S_{44} \quad (5a)$$

and

$$\theta_{13} = \theta_{14} \pm \frac{\pi}{2} \cdot \quad (5b)$$

In terms of small aperture approximation a possible solution for these equations was shown to be

$$M_x = M_z = M \quad (18a)$$

$$\cos\frac{\pi x_0}{a} = \frac{2a}{\lambda_{gr0}} \sin\frac{\pi x_0}{a} \cdot \quad (18b)$$

Since x_0 (distance from the aperture center to the wall of the rectangular waveguide) can be adjusted, (18b) may always be fulfilled, provided that there are no space limitations; therefore, "efficient" coupling apertures are desirable, i.e., apertures with a large M for a given linear dimension. There are many symmetrical shapes which might satisfy (18a) and (18b); among these the following were investigated: circular holes, square holes, and cross slots. For a given $|S_{33}|$ these different aperture shapes did not approximate (18a) and (18b) with the same quality of approximation as might be expected because of the approximative nature of small aperture theory. Square apertures appeared to yield the best approximation and at the same time were quite efficient.

Improvements

Since the results of the preliminary tests were encouraging, further studies were made to improve the characteristics of this structure. Major effort was aimed at improving the return loss and at providing a continuous adjustment of ∂ i.e., a continuous adjustment of the delay shape (11), since this would be an extremely valuable feature for any practical delay equalization of microwave filters with this equalizer.

First, it was observed, that some models exhibited lower return losses in the vicinity of the resonance frequency than others. This was caused by asymmetries of the structure which result in coupling between the two linear polarized waves in the cavity, which in turn spoils the perfect cancellation of the reflected waves around the resonance frequency. After attempts to correct this situation by mechanical precision proved impractical, a tuning screw C (Fig. 5) was introduced in the side wall of the cavity to compensate electrically for all mechanical asymmetries. With it and reasonable mechanical workmanship all equalizers could be adjusted to have return losses in excess of 40 dB in the vicinity of the resonance frequency.

The most notable improvement, however, was afforded by introducing a rather large diameter (0.5625 inch) tuning screw (D in Fig. 5) in the bottom wall of the rectangular waveguide close to the side wall. With a specific penetration of this screw and an associated small adjustment of x_0 it was possible to obtain return losses in excess of 40 dB for all equalizers for a band of ± 200 MHz around the resonance frequency of the cavity. Most importantly, however, it was found that this tuning screw D provided the desired continuous adjustability of ∂, i.e., a continuous adjustment of the delay shape. By deviating the value of x_0 and the penetration of screw D, from those values which yield the most broadband return loss, the delay shape can be changed considerably while maintaining a return loss in excess of 40 dB over a band of ± 100 MHz around the resonance frequency. A very rough physical explanation of this behavior in terms of small aperture theory can be given as follows. The introduction of the large diameter tuning screw below the coupling hole increases the intensity of both the transversal and the longitudinal component of the local magnetic field in the waveguide at the coupling hole, similar to a decrease of the waveguide height. Therefore, both $|S_{13}|$ and $|S_{14}|$ are increased, resulting in an increased efficiency of the coupling hole. In addition, by continuously varying the penetration of the screw, both $|S_{13}|$ and $|S_{14}|$ can be varied continuously, resulting in a continuous variation of the delay shape. However, the longitudinal magnetic field component is increased slightly more than the transversal component. Therefore, a small correction of the transversal position of the coupling hole is required in order to maintain a high return loss. Fig. 6 shows a typical range of adjustment. Since the equalizer is intended to equalize narrow band microwave bandpass filters (3 dB points typically at ± 14 MHz) the more restricted band of ± 100 MHz is still entirely adequate.

Performance as a Delay Equalizer, Temperature Influence

Delay: With the aid of a delay display measurement set a 5-cavity maximally flat bandpass filter tuned at 3710 MHz (3 dB points at ± 14 MHz) was equalized by a single equalizer of the configuration shown in Fig. 5. Fig. 8 is a photograph of this equalizer. Both the unequalized and the equalized delay are presented in Fig. 7. It is seen that no residual delay distortion could be observed for the equalized curve within ± 5.5 MHz of the center frequency. The equalizer adds about 20 ns of absolute delay and no difference could be found between the return loss of the filter and the return loss of the filter-equalizer assembly.

Losses: The dissipation loss of a typical equalizer was 0.308 dB at center frequency. This may be compared with the value 0.104 dB, which is obtained from (16). The appar-

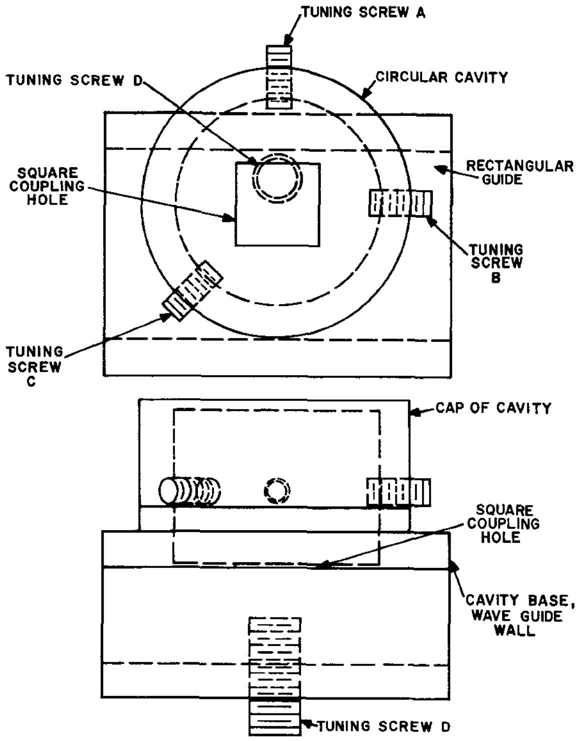

Fig. 5. Improved model of the delay equalizer.

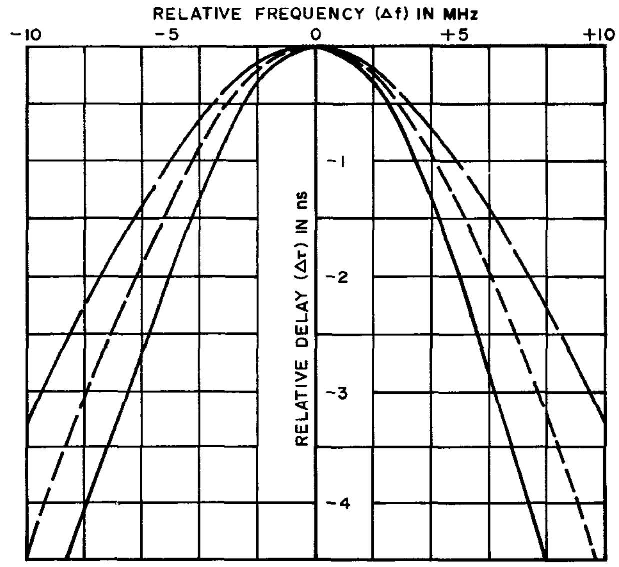

Fig. 6. Range of continuous adjustment of a delay curve ($f_0 = 3950$ MHz, aperture size 1.04 inch).

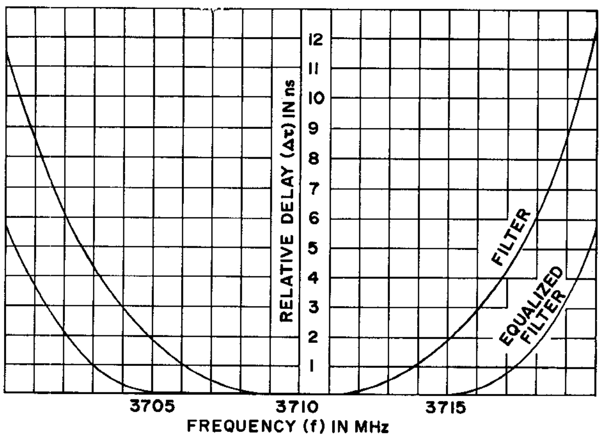

Fig. 7. Relative delay curves for a filter and an equalized filter.

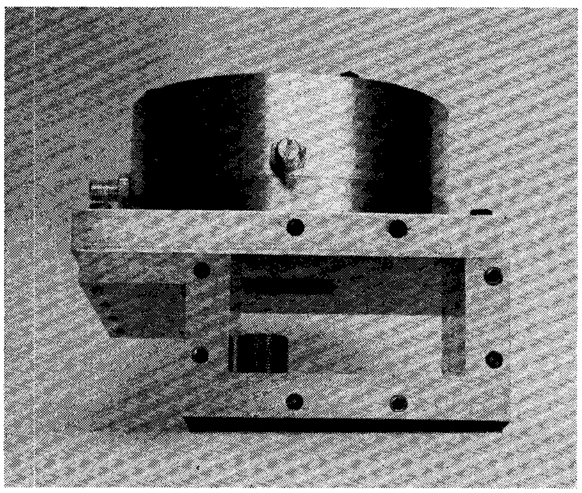

Fig. 8. Photograph of a typical delay equalizer.

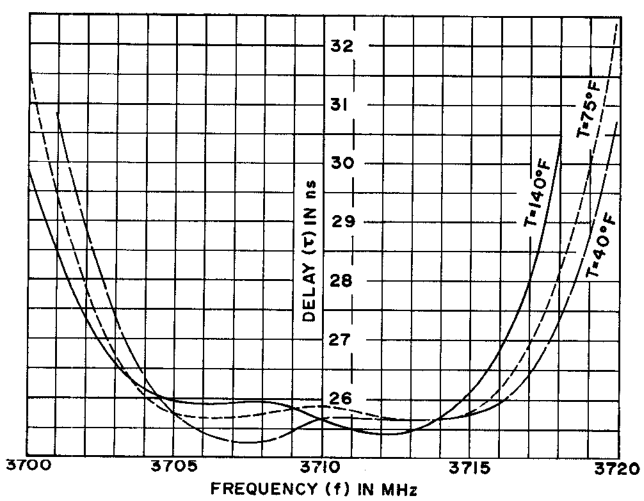

Fig. 9. Thermal behavior of the delay shape of a copper filter with a brass equalizer.

ent discrepancy is believed to be due to surface roughness, contact problems, and concentration of currents at the tuning screws; although it could also be due to the approximations involved in calculating the dissipation losses.

Temperature: Because of the existence of two spatial orthogonal modes in the cavity, perfect balance is required for a good return loss which necessitates that this balance must not be upset by temperature variations. An equalizer made out of brass was tuned at room temperature and its return loss was measured at 40 and 140°F. No serious return loss change (≥ 40 dB) was observed. This test was made for different penetrations of screw D, i.e., for different adjustments of the delay shape.

It may be concluded from these tests that the balance of the equalizer is not upset by temperature variations, however, the delay curve shifts in center frequency, when the temperature is changed. Since the delay curve of a bandpass filter also shifts in a similar manner, it should be possible to design the equalizer such that the two delay curves keep compensating each other over a limited temperature range. Therefore, a second temperature test was performed on a 5-cavity maximally flat copper bandpass filter in cascade with a brass equalizer. The delay distortion was roughly equalized at room temperature and the resulting delay was measured at room temperature and at 40 and 140°F. These three delay curves are presented in Fig. 9. They show an overall shift in frequency and also some degradation of the equalization, the latter indicating that filter and equalizer did not have the same rate of thermal expansion. However, the degradation is not too serious and it is believed that a better thermal behavior may be obtained by carefully choosing the material of the equalizer. It may be pointed out that this will not, however, eliminate the overall shift in frequency of the equalized delay. Removal of this shift appears to be possible only by using a material with a low coefficient of thermal expansion (such as invar) for both filter and equalizer.

Design Data

Since it would be quite difficult to compute $|S_{13}|$ or $|S_{33}|$ for a given aperture especially in the presence of tuning screw D (Fig. 5), it was decided to obtain the necessary design data from measurements. This information is presented in Figs. 10 through 12. The curves show the relative delay $\Delta\tau$ of equalizers with various aperture sizes centered around three frequencies (3710, 3950, and 4170 MHz) in the frequency band from 3.7 to 4.2 GHz. The aperture sizes chosen should provide adequate design information for the equalization of most 5-cavity narrow band bandpass filters. In all cases the equalizers were tuned to yield the most broadband return loss. The common mechanical dimensions were:

Main Waveguide—2.290 by 1.145 inches
Cavity Diameter—2.7 inches
Thickness of the Coupling Plate—0.025 inch
Diameter of Screw D—0.5625 inch
Aperture Shape—Square

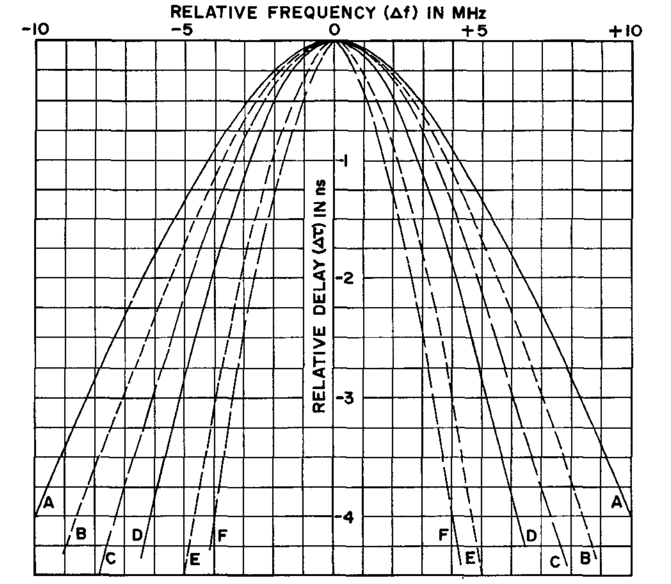

Fig. 10. Measured relative delay for equalizers with various aperture sizes (f_0=3710 MHz). In inches A=1.10, B=1.08, C=1.06, D=1.04, E=1.02, and F=1.

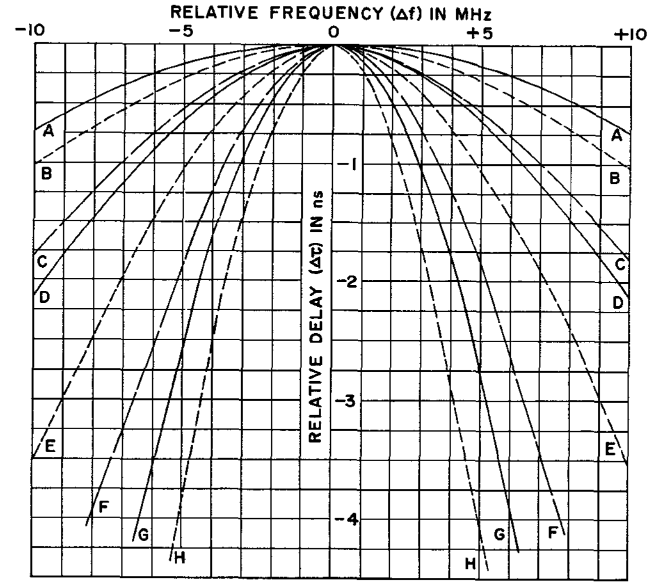

Fig. 12. Measured relative delay for equalizers with various aperture size (f_0=4170 MHz). In inches A=1.06, B=1.04, C=1.02, D=1.00, E=0.98, F=0.96, G=0.94, and H=0.92.

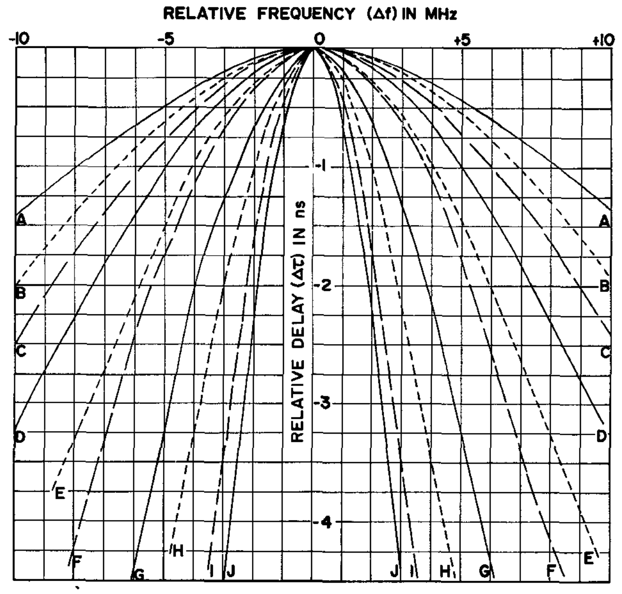

Fig. 11. Measured relative delay for equalizers with various aperture size (f_0=3950 MHz). In inches A=1.10, B=1.08, C=1.06, D=1.04, E=1.02, F=1.00, G=0.98, H=0.96, I=0.94, and J=0.92.

IV. Conclusion

The proposed structure has been shown to be very practical for the delay equalization of microwave bandpass filters in terms of size, loss, and complexity (cost). It is particularly convenient if some fine adjustment of the delay shape is needed. Obviously this adjustability also reduces the required mechanical precision by a considerable amount and consequently helps reducing the cost. Very good matching can be achieved. As a result of this, no isolator is required etween the filter and the equalizer.

Although some of the theoretical treatment is based on a small aperture approximation, the design information presented in the graphs was obtained from measurements and hence is free from any approximation. Many equalizers have been designed and built using these graphs and they work very well.

The proposed equalizer has a limited capability of delay equalization because it is only a one-section symmetrical lattice network. For wider delay equalization, more than one section has to be used. Because of their allpass nature, many sections can be cascaded directly.

Appendix

Mathematical Derivation of the Equivalent Circuit and Its Allpass Characteristic

First, the properties of the junction shown in Fig. 2 are investigated. Because of the degeneration of the TE_{11} eigenvalue in the circular waveguide, the junction can be considered to have four ports. In order to utilize the inherent symmetry, the eigenfunctions (polarizations) and reference planes are chosen as shown in Fig. 2. The following relations are then seen to be true:

$$S_{11} = S_{22}$$
$$S_{13} = S_{23}$$
$$S_{14} = -S_{24}$$
$$S_{34} = S_{43} = 0.$$

These equations together with reciprocity result in the scattering matrix

$$S = \begin{bmatrix} S_{11} & S_{12} & S_{13} & S_{14} \\ S_{12} & S_{11} & S_{13} & -S_{14} \\ S_{13} & S_{13} & S_{33} & 0 \\ S_{14} & -S_{14} & 0 & S_{44} \end{bmatrix}. \tag{19}$$

Now port 3 and port 4 are terminated by short circuits a distance l_3 and l_4 away from the ports. Then

$$a_3 = -e^{-2j\beta l_3} b_3,$$
$$a_4 = -e^{-2j\beta l_4} b_4 \tag{20}$$

where β is the phase constant of the TE_{11} modes in the circular waveguide. Introduction of (20) into (19) yields

$$\begin{pmatrix} b_1 \\ b_2 \end{pmatrix} = \begin{pmatrix} S_r & S_t \\ S_t & S_r \end{pmatrix} \begin{pmatrix} a_1 \\ a_2 \end{pmatrix} \tag{21}$$

with

$$S_r = S_{11} - \frac{S_{13}^2}{S_{33} + e^{2j\beta l_3}} - \frac{S_{14}^2}{S_{44} + e^{2j\beta l_4}},$$
$$S_t = S_{12} - \frac{S_{13}^2}{S_{33} + e^{2j\beta l_3}} + \frac{S_{14}^2}{S_{44} + e^{2j\beta l_4}}. \tag{22}$$

Since the junction is lossless, it is

$$|S_{11}|^2 + |S_{12}|^3 + |S_{13}|^2 + |S_{14}|^2 = 1$$
$$2|S_{13}|^2 + |S_{33}|^2 = 1$$
$$2|S_{14}|^2 + |S_{44}|^2 = 1$$
$$S_{11}S_{12}^* + S_{12}S_{11}^* + |S_{13}|^2 - |S_{14}|^2 = 0$$
$$S_{11}S_{13}^* + S_{12}S_{13}^* + S_{13}S_{33}^* = 0$$
$$S_{11}S_{14}^* - S_{12}S_{14}^* + S_{14}S_{44}^* = 0. \tag{23}$$

The symbol * denotes the complex conjugate value. Using the conventional notation

$$S_{ij} = |S_{ij}| e^{j\theta_{ij}}$$

and operating on (22) with the aid of (23) it is obtained

$$S_r - S_t = -e^{2j(\theta_{14} - \theta_{44} + \beta l_4)} \frac{S_{44} + e^{2j(\theta_{44} - \beta l_4)}}{S_{44} + e^{2j\beta l_4}},$$
$$S_r + S_t = -e^{2j(\theta_{13} - \theta_{33} + \beta l_3)} \frac{S_{33} + e^{2j(\theta_{33} - \beta l_3)}}{S_{33} + e^{2j\beta l_3}}. \tag{24}$$

Since

$$\frac{S_{33} + e^{2j(\theta_{33} - \beta l_3)}}{S_{33} + e^{2j\beta l_3}} = \frac{|S_{33}| + e^{j(\theta_{33} - 2\beta l_3)}}{|S_{33}| + e^{-j(\theta_{33} - 2\beta l_3)}} = e^{2j\phi}$$

where

$$\phi = \arctan \frac{\sin(\theta_{33} - 2\beta l_3)}{|S_{33}| + \cos(\theta_{33} - 2\beta l_3)} \tag{25}$$

and since

$$\frac{S_{44} + e^{2j(\theta_{44} - \beta l_4)}}{S_{44} + e^{2j\beta l_4}} = e^{2j\psi}$$

where

$$\psi = \arctan \frac{\sin(\theta_{44} - 2\beta l_4)}{|S_{44}| + \cos(\theta_{44} - 2\beta l_4)} \tag{26}$$

(24) may be operated on to yield

$$S_r = \frac{-1}{2}\left[e^{2j(\theta_{13} - \theta_{33} + \phi + \beta l_3)} + e^{2j(\theta_{14} - \theta_{44} + \psi + \beta l_4)}\right],$$
$$S_t = \frac{-1}{2}\left[e^{2j(\theta_{13} - \theta_{33} + \phi + \beta l_3)} - e^{2j(\theta_{14} - \theta_{44} + \psi + \beta l_4)}\right]. \tag{27}$$

With the standard transformation

$$Z = (1 - S)^{-1}(1 + S)$$

the normalized impedance matrix

$$Z = \begin{pmatrix} z_{11} & z_{12} \\ z_{12} & z_{11} \end{pmatrix}$$

is obtained where

$$z_{11} = \frac{1}{2}\left(\frac{1 - e^{2j(\theta_{13} - \theta_{33} + \phi + \beta l_3)}}{1 + e^{2j(\theta_{13} - \theta_{33} + \phi + \beta l_3)}} + \frac{1 - e^{2j(\theta_{14} - \theta_{44} + \psi + \beta l_4)}}{1 + e^{2j(\theta_{14} - \theta_{44} + \psi + \beta l_4)}}\right),$$
$$z_{12} = \frac{1}{2}\left(\frac{1 - e^{2j(\theta_{13} - \theta_{33} + \phi + \beta l_3)}}{1 + e^{2j(\theta_{13} - \theta_{33} + \phi + \beta l_3)}} - \frac{1 - e^{2j(\theta_{14} - \theta_{44} + \psi + \beta l_4)}}{1 + e^{2j(\theta_{14} - \theta_{44} + \psi + \beta l_4)}}\right). \tag{28}$$

It is readily seen that this impedance matrix may be represented by the symmetrical lattice network shown in Fig. 3 with the following lattice impedances:

$$Z_a = -j \tan(\theta_{13} - \theta_{33} + \phi + \beta l_3),$$
$$Z_b = -j \tan(\theta_{14} - \theta_{44} + \psi + \beta l_4). \tag{29}$$

It is well known that the symmetrical lattice network of Fig. 3 is a matched allpass, if

$$Z_a Z_b = 1. \tag{30}$$

As may be seen from (29) a solution for (30) is

$$S_{33} = S_{44} \tag{31a}$$

$$\theta_{13} = \theta_{14} \pm \frac{\pi}{2} \tag{31b}$$

and

$$l_3 = l_4 = l \tag{31c}$$

Equation (31c) can readily be fulfilled. An exact evaluation of the scattering matrix elements in order to fulfill (31a) and (31b) would be quite difficult. However, an approximation based on small aperture theory[4] is easy to obtain.

In order to characterize a given coupling aperture by small aperture theory, the aperture is usually described by an electric polarizability and by two magnetic polarizabilities along two axes. Let M_x and M_z be the magnetic polarizabilities along the x and z axes respectively, (Fig. 2). Then the desired elements of the scattering matrix can be expressed in the following way:

$$S_{13} = C_1 M_z H_{z1} H_{z3}$$
$$S_{14} = C_1 M_x H_{x1} H_{x4}$$
$$S_{33} = C_2(M_x H_{x3} H_{x3} + M_z H_{z3} H_{z3})$$
$$S_{44} = C_2(M_x H_{x4} H_{x4} + M_z H_{z4} H_{z4}).$$

C_1 and C_2 are constants depending upon frequency, dimensions other than the aperture dimensions, and normalization of the field intensities. The field components are the components of the unperturbed normalized eigenfunctions present at the ports 1, 3 and 4 evaluated in the center of the aperture.

A choice which satisfies (31a) and (31b) is to choose a coupling aperture with $M_x = M_z = M$ and to locate the aperture at the center of the cavity end plate and a distance x_0 from the side wall of the rectangular waveguide, so that $|H_{x1}| = |H_{z1}|$ (Fig. 2). At the center of the cavity

$$H_{x3} = H_{z4} = 0$$

and

$$H_{z3} = H_{x4} = H_r$$

are valid. This means that (31a) is fulfilled at all frequencies. Since

$$H_{z1} = \cos \frac{\pi x_0}{a}$$

and

$$H_{x1} = -j \frac{2a}{\lambda_{gr}} \sin \frac{\pi x_0}{a}$$

(a is the width of the rectangular waveguide and λ_{gr} is the guide wavelength of the TE_{10} made in this guide) x_0 has to be chosen such that at the center frequency f_0 of the equalizer $[\lambda_{gr0} = \lambda_{gr}(f_0)]$

$$\cos \frac{\pi x_0}{a} = \frac{2a}{\lambda_{gr0}} \sin \frac{\pi x_0}{a} \cdot \qquad (32)$$

This results in

$$\theta_{13} = \theta_{14} + \frac{\pi}{2} \cdot$$

Concerning the frequency dependency a closer examination shows, that

$$S_{13} = D_1 M \sqrt{\frac{\lambda_{gr}}{\lambda_g}}$$

$$S_{14} = -jD_1 M \frac{\lambda_{gr0}}{\sqrt{\lambda_{gr}\lambda_g}}$$

and

$$S_{33} = S_{44} = -\frac{1}{1 + j\dfrac{D_2 M}{\lambda_g}} \cdot$$

Here D_1 and D_2 are positive real constants depending only upon the dimensions of the two waveguides. Thus, not only (31a) but also (31b) is fulfilled independent of frequency. Therefore, Z_a and Z_b satisfy the condition (30) throughout the frequency range and (27) can be simplified to read

$$S_r = 0,$$
$$S_t = -e^{2j(\theta_{13} - \theta_{33} + \phi + \beta l)}. \qquad (33)$$

The above expressions for S_{13} and S_{33} also show that θ_{13}, θ_{33}, and $|S_{33}|$ can be assumed to be approximately constant for a frequency band of ≤ 1 percent relative bandwidth. E.g. for a typical value $\partial = 1 - |S_{33}| = 0.025$, for a band of a 1 percent relative bandwidth, and for typical values $(\lambda_g/\lambda)^2 = 1.3$, $(\lambda_{gr}/\lambda)^2 = 1.5$ the maximum variations of θ_{13}, θ_{33}, and $|S_{33}|$ within this band are

$$\Delta\theta_{13} = 0$$

$$\Delta\theta_{33} = 0.17 \text{ degrees}$$

and

$$\Delta |S_{33}| = 6.5 \cdot 10^{-4}.$$

References

[1] D. Merlo, "Development of group-delay equalizers for 4 Gc/s," *Proc. IEE* (London), vol. 112, pp. 289–295, February 1965.

[2] L. C. Tillotson, "Microwave filters," U. S. Patent 2 795 763, June 11, 1957.

[3] S. B. Cohn, "Microwave dual mode resonator apparatus for equalizing and compensating for nonlinear phase angle or time delay characteristics of other components," U. S. Patent 3 277 403, October 4, 1966.

[4] H. A. Bethe, "Theory of diffraction by small holes," *Phys. Rev.*, vol. 66, pp. 163–182, October 1944.

[5] H. F. Mayer, "Ueber die Daempfung von Siebketten im Durchlaessigkeitsbereich" (in German), *Elektrische Nachrichtentechnik*, vol. 2 pp. 335–338, 1925.

[6] C. G. Montgomery, *Principle of Microwave Circuits.* New York: McGraw-Hill, 1951.

[7] I. G. Wilson, C. W. Schramm and J. P. Kinzer, "High *Q* resonant cavities for microwave testing," *Bell Sys. Tech. J.*, vol. 25, pp. 408–433, 1946.